Ultrasound in Med. & Biol., Vol. 32, No. 11, pp. 1793–1804, 2006
Copyright © 2006 World Federation for Ultrasound in Medicine & Biology
Printed in the USA. All rights reserved
0301-5629/06/$–see front matter

ELSEVIER

doi:10.1016/j.ultrasmedbio.2006.03.011

● *Original Contribution*

THRESHOLD ESTIMATION OF ULTRASOUND-INDUCED LUNG HEMORRHAGE IN ADULT RABBITS AND COMPARISON OF THRESHOLDS IN MICE, RATS, RABBITS AND PIGS

WILLIAM D. O'BRIEN, JR.,* YAN YANG,† DOUGLAS G. SIMPSON,† LEON A. FRIZZELL,* RITA J. MILLER,* JAMES P. BLUE, JR.,* and JAMES F. ZACHARY‡

*Bioacoustics Research Laboratory, Department of Electrical and Computer Engineering, University of Illinois, Urbana, IL; †Department of Statistics, University of Illinois, Champaign, IL; and ‡Department of Pathobiology, University of Illinois, Urbana, IL, USA

(*Received* 11 *November* 2005, *in final form* 5 *March* 2006)

Abstract—The objective of this study was to assess the threshold and superthreshold behavior of ultrasound (US)-induced lung hemorrhage in adult rabbits to gain greater understanding about species dependency. A total of 99 76 ± 7.6-d-old 2.4 ± 0.14-kg New Zealand White rabbits were used. Exposure conditions were 5.6-MHz, 10-s exposure duration, 1-kHz PRF and 1.1-μs pulse duration. The *in situ* (at the pleural surface) peak rarefactional pressure, $p_{r(in\ situ)}$, ranged between 1.5 and 8.4 MPa, with nine acoustic US exposure groups plus a sham exposure group. Rabbits were assigned randomly to the 10 groups, each with 10 rabbits, except for one group that had nine rabbits. Rabbits were exposed bilaterally with the order of exposure (left then right lung, or right then left lung) and acoustic pressure both randomized. Individuals involved in animal handling, exposure and lesion scoring were blinded to the exposure condition. Probit regression analysis was used to examine the dependence of the lesion occurrence on *in situ* peak rarefactional pressure and order of exposure (first *vs.* second). Likewise, lesion depth and lesion root surface area were analyzed using Gaussian tobit regression analysis. Neither probability of a lesion nor lesion size measurements was found to be statistically dependent on the order of exposure after the effect of $p_{r(in\ situ)}$ was considered. Also, a significant correlation was not detected between the two exposed lung sides on the same rabbit in either lesion occurrence or size measures. The $p_{r(in\ situ)}$ threshold estimates (in MPa) were similar to each other across occurrence (3.54 ± 0.78), depth (3.36 ± 0.73) and surface area (3.43 ± 0.77) of lesions. Using the same experimental techniques and statistical approach, great consistency of thresholds was demonstrated across three species (mouse, rat and rabbit). Further, there were no differences in the biologic mechanism of injury induced by US and US-induced lesions were similar in morphology in all species and age groups studied. The extent of US-induced lung damage and the ability of the lung to heal led to the conclusion that, although US can produce lung damage at clinical levels, the degree of damage does not appear to be a significant medical problem. (E-mail: wdo@uiuc.edu) **© 2006 World Federation for Ultrasound in Medicine & Biology.**

Key Words: **Ultrasound bioeffects, Rabbit lung, Pulsed ultrasound, Lung hemorrhage, Damage threshold.**

INTRODUCTION

Clinical diagnostic ultrasound (US) continues to be one of the most widely used and safest imaging modalities available in medical practice. However, concerns for its safety continue to be raised and addressed by members of the bioeffects research community (WFUMB 1998; AIUM 2000). These concerns are the result of numerous US-induced lung hemorrhage studies in mice, rats, rabbits, monkeys and pigs at exposure conditions similar to those used for scanning in humans (Child et al. 1990; Hartman et al. 1990; Penney et al. 1993; Raeman et al. 1993, 1996; Frizzell et al. 1994, 2003; Tarental and Canfield 1994; Zachary and O'Brien 1995; Harrison et al. 1995; Baggs et al. 1996; Holland et al. 1996; O'Brien and Zachary 1997; Dalecki et al. 1997a, 1997b; WFUMB 1998; AIUM 2000; O'Brien et al. 2000, 2001a, 2001b, 2003a, 2003b, 2005; Kramer et al. 2001; Zachary et al. 2001a, 2001b).

The study reported herein evaluates the US-induced lung hemorrhage in adult rabbits. We previously examined lung hemorrhage in New Zealand White rabbits

Address correspondence to: William D. O'Brien, Jr., Bioacoustics Research Laboratory, Department of Electrical and Computer Engineering, University of Illinois, 405 North Mathews, Urbana, IL 61801. E-mail: wdo@uiuc.edu

using a commercial diagnostic US imaging system (O'Brien and Zachary 1997). The purpose of that study was to assess experimentally the question of whether the mechanical index (MI) is an equivalent or better indicator of nonthermal bioeffect risk than $I_{SPPA.3}$ (derated spatial peak, pulse average intensity). The study showed that the MI was a better indicator of rabbit lung damage than either the $I_{SPPA.3}$ or $p_{r.3}$ (derated peak rarefactional pressure) (FDA 1994). The study did not estimate lesion thresholds and, therefore, this contribution performs threshold estimation in rabbits.

Further, because there have been other threshold studies conducted using the same experimental and analysis protocols, but with different species, the rabbit threshold findings are compared against adult mouse (Zachary et al. 2001a) and adult rat (Zachary et al 2001a; O'Brien et al. 2001b), as well as pig threshold findings (O'Brien et al. 2003a). These threshold findings represent a unique species-dependent dataset that is not available for any other *in vivo* US-induced biologic effect. One of the principal goals of our US-induced lung hemorrhage has been a thorough analysis of lung damage across species. The purpose of a thorough evaluation of species dependency is to hopefully provide a basis by which an estimate is made as to whether this US-induced lung damage is a medically significant problem in humans.

MATERIALS AND METHODS

Exposimetry

The exposimetry and calibration procedures have been described previously in detail (Frizzell et al. 2003; O'Brien et al. 2001b, 2003a, 2003b, 2005; Zachary et al. 2001a, 2001b). Ultrasonic exposures were conducted using a focused f/2, 19-mm-diameter, lithium niobate ultrasonic transducer (Valpey Fisher, Hopkinton, MA, USA). Water-based (degassed, 22°C) pulse-echo ultrasonic field distribution measurements were performed according to established procedures (Raum and O'Brien 1997; Zachary et al. 2001a) and yielded a center frequency of 5.6 MHz, a fractional bandwidth of 11%, a focal length of 38 mm, a −6-dB focal beamwidth of 510 μm and a −6-dB depth of focus of 6.5 mm.

An automated procedure, based on established standards (AIUM/NEMA 1998, 2004), was used routinely to calibrate the US fields (Sempsrott and O'Brien 1999; Zachary et al. 2001a). Briefly, the source transducer's drive voltage was supplied by a RAM5000 (Ritec, Inc., Warwick, RI, USA). A calibrated PVDF membrane hydrophone (Marconi model Y-34-6543, Chelmsford, UK) was mounted to the computer-controlled micropositioning system (Daedal, Inc., Harrisburg, PA, USA). The hydrophone's signal was digitized with an oscilloscope (500 MS/s, LeCroy model 9354TM, Chestnut Ridge, NY, USA), the output of which was fed to the same computer (Dell Pentium II, Dell Corporation, Round Rock, TX, USA) that controlled the positioning system. Off-line processing (MATLAB®, Mathworks, Inc., Natick, MA, USA) yielded the water-based peak rarefactional pressure $p_{r(\text{in vitro})}$ and the water-based peak compressional pressure $p_{c(\text{in vitro})}$. The MI was also determined from the measurement procedure (AIUM/NEMA 2004): the $MI = p_{r.3}/\sqrt{f_c}$, where $p_{r.3}$ is the derated (0.3 dB/cm-MHz) peak rarefactional pressure (in MPa) and f_c is the center frequency (in MHz). The MI is reported because it is a regulated quantity (FDA 1997) of diagnostic US systems and its value is available to system operators. Thus, there is value to provide the MI for each of our exposure settings to give general guidance to manufacturers and operators as to the levels which we used in this study. Further, as seen from the MI definition, it is a quantity that must be determined from the water-based measurement process, and cannot be determined from $p_{r(\text{in vivo})}$.

Independent calibrations were performed weekly on the 5.6-MHz focused transducer during the period of the experiment. One set of calibrations was performed before exposures were initiated each week, and one set of calibrations was performed after exposures were concluded for each week. Relative standard deviations $\frac{\text{standard deviation}}{\text{mean}}$ of $p_{r(\text{in vitro})}$ and $p_{c(\text{in vitro})}$ were 6% and 10% ($n = 15$), respectively. The pulse duration was also measured (AIUM/NEMA 1998) at every calibration and its mean value (relative standard deviation) was 1.1 (8%) μs.

To estimate the *in situ* (at the pleural surface) peak rarefactional and compressional pressures, an independent study was conducted to measure the attenuation coefficient [insertion loss (IL) as a function of intercostal tissue thickness] in New Zealand White rabbits. The same procedures were used as those in previously published papers on intercostal attenuation coefficient estimates (Teotico et al. 2001; Miller et al. 2002; Towa et al. 2002). IL data were acquired from 16 rabbits between the frequencies 1.34 and 3.78 MHz and acquired from 10 rabbits between the frequencies 4.15 and 8.67 MHz, all at a tissue temperature of 37°C (Fig. 1). For the study reported herein, an attenuation coefficient of 10.2 dB/cm (std = 2.2 dB/cm) at 5.6 MHz was used.

The *in situ* peak rarefactional and compressional pressures were estimated for each rabbit from

$$p_{r(\text{in situ})} = p_{r(\text{in virto})} e^{-(A \cdot x)} \quad (1a)$$

and

$$p_{c(\text{in situ})} = p_{c(\text{in virto})} e^{-(A \cdot x)}, \quad (1b)$$

respectively, where $p_{r(\text{in vitro})}$ and $p_{c(\text{in vitro})}$ are defined

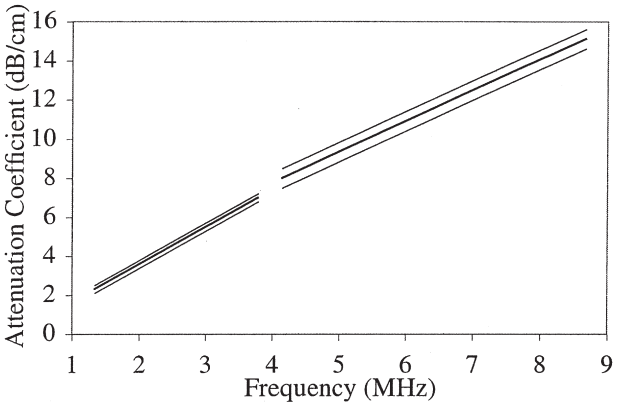

Fig. 1. Attenuation coefficient regression functions (linear regression lines ± 95% confidence band for the regression line) as a function of frequency for the intercostal tissues of New Zealand White rabbits at 37°C. The lower frequency attenuation coefficient data were derived from 16 rabbit chest walls and the higher frequency data were derived from 10 rabbit chest walls.

above and A is the intercostal tissue attenuation coefficient. The measured individual intercostal tissue thicknesses, x, were used in eqns (1a) and (1b) to calculate $p_{r(in\ situ)}$ and $p_{c(in\ situ)}$ (Table 1).

Animals

The experimental protocol was approved by the Institutional Animal Care and Use Committee, University of Illinois, and satisfied all campus and National Institutes of Health rules for the humane use of laboratory animals. Animals were housed in an Association for Assessment and Accreditation of Laboratory Animal Care (Rockville, MD, USA)-approved animal facility and provided with food and water *ad lib*.

There were a total of 99 76 ± 7.6-d-old (mean ± SD) New Zealand White rabbits (Myrtle's Rabbitry, Thompson Station, TN, USA) [weight: 2.4 ± 0.14 kg; chest wall thickness: 5.6 ± 0.32 mm (first exposed) and 5.6 ± 0.33 mm (second exposed)]. Animal weights were measured at the time of the experiment and animal ages were determined from exact birth dates.

Rabbits were assigned randomly to 10 acoustic pressure levels (Table 1), each with 10 rabbits, except one group that had nine rabbits. The individuals involved in rabbit handling, exposure, necropsy and lesion scoring were blinded to the exposure condition. The exposure condition for each rabbit was revealed only after the final results were tabulated.

Rabbits were anesthetized with ketamine hydrochloride (50.0 mg/kg) and xylazine (10.0 mg/kg)

Table 1. Mean values of the *in situ* (at the pleural surface) peak rarefactional pressure $p_{r(in\ situ)}$ and *in situ* peak compressional pressure $p_{c(in\ situ)}$ and their respective lesion occurrence and mean (SEM) values of the lesion depth and surface area

Number of animals	$P_{r(in\ situ)}$ (MPa)	$P_{c(in\ situ)}$) (MPa)	Mechanical index	% Lesion occurrence	Mean (SEM) lesion depth (mm)	Mean (SEM) lesion area (mm^2)
Exposure order: first lung exposed						
10 (sham)	0.34	0.33	0.12	10	0.045 (0.045)	0.30 (0.30)
10	1.5	2.1	0.54	0	—	—
10	2.0	3.2	0.72	0	—	—
10	2.7	5.4	0.96	0	—	—
10	3.1	6.7	1.1	10	0.010 (0.010)	0.22 (0.22)
10	4.3	9.5	1.5	10	0.16 (0.16)	0.78 (0.78)
10	5.3	11.4	1.9	30	0.40 (0.21)	1.36 (0.85)
9	6.7	13.9	2.4	33	0.86 (0.45)	3.16 (1.59)
10	7.8	14.8	2.8	50	1.28 (0.44)	5.76 (2.11)
10	8.4	15.2	3.0	70	1.64 (0.37)	7.28 (1.71)
Exposure order: second lung exposed						
10 (sham)	0.34	0.34	0.12	10	0.21 (0.21)	0.25 (0.25)
10	1.5	2.1	0.54	0	—	—
10	2.0	3.2	0.72	0	—	—
10	2.7	5.4	0.96	0	—	—
10	3.1	6.6	1.1	20	0.43 (0.31)	3.88 (3.49)
10	4.3	9.4	1.5	0	—	—
10	5.3	11.4	1.9	10	0.17 (0.17)	0.20 (0.20)
9	6.7	13.8	2.4	11	0.21 (0.21)	0.77 (0.77)
10	7.8	14.8	2.8	50	1.02 (0.36)	5.11 (1.73)
10	8.4	15.2	3.0	60	1.33 (0.42)	8.84 (3.32)

All rabbits were exposed to pulsed US (1-kHz pulse repetition frequency, 10-s exposure duration, 1.1-μs pulse duration). The sham exposure conditions used a pulse repetition frequency of 10 Hz. Mean values of the mechanical index (MI), as measured according to the applicable standard (AIUM/NEMA 2004), are provided, because the MI is a regulated quantity of diagnostic US equipment.

administered subcutaneously. The skin of the thorax (both sides) was shaved with an electric clipper, followed by a depilatory agent (Nair®, Carter-Wallace, Inc., New York, NY, USA) to maximize sound transmission. A black dot was placed on the skin at approximately the fifth to sixth intercostal space on both sides, to guide the lateral positioning of the ultrasonic beam. Anesthetized rabbits were placed in right or left lateral recumbency and a stand-off tank was positioned in contact with the skin. Mineral oil was used as the coupling agent on the skin surface. All rabbits were exposed bilaterally. The US transducer, placed in the stand-off tank that contained degassed water at 30°C, was aligned with the black dot before each exposure. The low-power pulse-echo capability of the exposure system (RAM5000, Ritec, Inc.) displayed on an oscilloscope was used to align the axial center of the focal region to within 1 mm of the lung surface (see Table 1 for sham levels). Also, the pulse repetition frequency was 10 Hz during this alignment procedure. Thus, the ultrasonic beam was approximately perpendicular to the skin at the position of the black dot, with the beam's focal region at the lateral surface of the lung and approximately normal to the lung's pleural surface. After either the left or right lung was exposed, the rabbit was turned over, the transducer realigned again as described above, and the rabbit's other lung exposed. Each rabbit was positioned on each side for 4 min. The time was kept consistent to prevent either side from collapsing more than the other. Also, the rabbits were kept in sternal recumbency while the depilatory agent was working. The acoustic pressure levels were the same for both the left and right lungs of each rabbit. The order (left then right lung, or right then left lung) was randomized, with an equal number of exposures for each order.

The distance between the transducer and the lung surface did not vary by more than 1 to 2 mm, because the water-filled stand-off tank was placed gently on the rabbit's lateral aspect, thus limiting chest expansion in that direction. The transducer's −6-dB depth of focus is 6.5 mm so the lung surface remained within the focal region as a function of the animal's breathing. Also, the orientation of the chest wall surface in contact with the water-filled stand-off tank did not visually change as a function of breathing. Because the chest wall surface and the lung surface track each other, the orientation between the beam axis and the pleural surface did not change.

Each lung was exposed to 5.6-MHz pulsed US with a pulse repetition frequency (PRF) of 1 kHz, an exposure duration (ED) of 10 s and a pulse duration (PD) of 1.1 μs. The 10-s ED was used to simulate incidental exposure to lung tissue, because, in clinical practice, the lung is generally not intentionally exposed to diagnostic US. After exposure, rabbits were euthanized under anesthesia with CO_2.

A midline incision was made to open the chest cavity. The left and right thoracic walls were opened and the thicknesses of the intercostal tissue (skin, fat, fascia, muscle and parietal pleura) were measured on both sides with a digital micrometer (accuracy: 10 μm; Mitutoyo Corp., Kawasaki, Kanagawa, Japan) at the locations of exposure. These chest wall measurements were used for later calculation of the *in situ* ultrasonic pressures at the visceral pleural surface (eqn (1)).

The lungs were removed from each rabbit and examined grossly for the presence or absence of a lesion and then photographed digitally. The base of the lesion originated at the visceral pleural surface and was elliptical in shape. The lesion extended into the lung parenchyma to form its apex at varied depths within the lung. A section of the lung where the lesion appeared, or the target area where the lesion would have appeared, was trimmed away from the lung, placed in a sterile 50-mL clear polypropylene centrifuge tube and then fixed by immersion in 10% neutral-buffered formalin for a minimum of 24 h. After total fixation, the elliptical dimensions of lung lesions at the visceral pleural surface were measured with a digital micrometer (accuracy: 10 μm), where "a" was the length of the semimajor axis and "b" was the length of the semiminor axis. The lesions were then bisected and the depth "d" of the lesion within the lung was measured. In animals where the depth of the lesion was not visually discernable, the depth was determined from measurements made on histologic sections with a slide micrometer. The surface area (πab) and volume (πabd/3) of the lesion were calculated for each lung. Each half of the bisected lesion was embedded in paraffin, sectioned at 5 μm, stained with hematoxylin and eosin and evaluated microscopically.

Statistics

The outcome variables were lesion occurrence and size (depth and surface area). The goals of the statistical analysis were to model the outcome variables and to estimate threshold acoustic pressures associated with occurrence and sizes. Lesion occurrence was recorded as a binary 0-1 outcome, with "0" indicating a nonlesion and "1" indicating a lesion. Lesion size measurements were positive numbers, except for zeros which corresponded to nonlesions. As each animal was exposed bilaterally, the two measures of an outcome variable on the same rabbit, one for each lung side, were potentially correlated, whereas observations from different rabbits were assumed independent because of the experimental design. The covariates of primary interest were $p_{r(\text{in situ})}$, denoted by Pr in the statistical models, and exposure

order ("1" denotes first lung exposed and "2" denotes second lung exposed), abbreviated by EO.

The binary outcomes of lesion occurrence were analyzed by a probit mixed model with a random effect for each animal to account for correlation between the outcomes from the two lung sides. In this model, the probability of a lesion was fitted as a standard normal distribution function of a linear mixed model with a random intercept (Pinheiro and Bates 1995). Let P_{ij} be the probability of a lesion for the j^{th} exposure on the i^{th} animal, $i = 1, \ldots, 89$, $j = 1, 2$ and denote Φ as the standard normal distribution function. The probit regression started with the following full-trend mixed model:

$$P_{ij}^{P} = \Phi(\gamma_0 + \gamma_1 Pr_{ij} + \gamma_2 EO_{ij} + \gamma_3 Pr_{ij} \times EO_{ij} + A_i), \quad (2)$$

where the superscript in P_{ij}^{P} denotes probit and the subscript indicates the levels of Pr and EO for the j^{th} exposure on animal i. γ_0 is the fixed intercept of the linear mixed model; γ_1, γ_2 and γ_3 are coefficients for Pr_{ij}, EO_{ij} and $Pr_{ij} \times EO_{ij}$ (interaction between Pr_{ij} and EO_{ij}), respectively, and A_i is the Gaussian random effect for the i^{th} rabbit, with mean 0 and variance a^2. After the full-trend mixed model (eqn (2)) was estimated, backward selection was used to determine whether the Pr × EO interaction and EO main effect could be removed from the model. The backward selection tests used the commonly-chosen 0.05 significance level.

The nonnegative lesion depth and root surface area ($\sqrt{\text{surface area}}$) were each analyzed by a Gaussian tobit mixed model. A Gaussian tobit model assumes that the observed effect corresponds to a latent normal variable censored below at zero. Hence, the median of the observed data (*i.e.*, lesion size) equals zero up to a threshold acoustic pressure (the ED50 to be introduced momentarily) and increases linearly above the threshold (Amemiya 1984). Denote Y_{ij} as the observed j^{th} size measure on animal i. The full-trend mixed model for lesion size is given by:

$$Y_{ij} = \max\{0, \beta_0 + \beta_1 Pr_{ij} + \beta_2 EO_{ij} + \beta_3 Pr_{ij} \times EO_{ij} + B_i + \varepsilon_{ij}\}, \quad (3)$$

for $i = 1, \ldots, 89$; $j = 1, 2$, where β_0 is the fixed intercept of the linear mixed model; β_1, β_2 and β_3 are coefficients for Pr_{ij}, EO_{ij} and $Pr_{ij} \times EO_{ij}$, respectively; B_i is the Gaussian random effect for the i^{th} rabbit with mean 0 and variance b^2; and ϵ_{ij} is the normally distributed random error with mean zero and variance σ^2. B_i and ϵ_{ij} were assumed to be independent of each other. The tobit mixed model (eqn (3)) implies that the probability of a lesion, conditional on the random effect B_i, is provided by

$$P_{ij}^{T} = P(Y_{ij} > 0) = \Phi\left(\frac{\beta_0 + \beta_1 Pr_{ij} + \beta_2 EO_{ij} + \beta_3 Pr_{ij} \times EO_{ij} + B_i}{\sigma}\right), \quad (4)$$

where the superscript in P_{ij}^{T} denotes tobit. Backward elimination was again used to select the final model, based on the full-trend tobit mixed model (eqn (3)). The probit mixed models for lesion occurrence and Gaussian tobit mixed models for lesion size were both estimated by maximum likelihood estimation implemented in the SAS procedure NLMIXED (Berk and Lachenbruch 2002).

After maximum likelihood estimates (MLEs) were obtained from the final probit mixed model and Gaussian tobit mixed models, the threshold acoustic pressures associated with certain incidence rates, such as 5% and 50% risks, were evaluated. The thresholds corresponding to 5% and 50% risk levels are usually called ED05 and ED50, meaning the effective doses associated with 5% and 50% risks, respectively. A detailed treatment of excess risk due to exposure for binary or nonnegative size data can be found in Simpson et al. (2004). Let P(x) denote the probability of lesion occurrence for Pr equal to x (where Pr is $p_{r(\text{in situ})}$), then P(0) corresponds to the background risk level and the excess risk due to exposure q is defined as

$$q = \frac{P(x) - P(0)}{1 - P(0)}. \quad (5)$$

For a probit mixed model $P(x) = P^{P}(x)$ is the final model selected from eqn (2) and averaged over the random effect A_i to give, in the absence of interaction and order-of-exposure effects:

$$P^{P}(x) = \Phi\left(\frac{\gamma_0 + \gamma_1 x}{\sqrt{1 + a^2}}\right). \quad (6)$$

For a Gaussian tobit mixed model, $P(x) = P^{T}(x)$ is the final model based on eqn (4) and averaged over the random effect B_i to give, in the absence of interaction and order-of-exposure effects:

$$P^{T}(x) = \Phi\left(\frac{\beta_0 + \beta_1 x}{\sqrt{\sigma^2 + b^2}}\right). \quad (7)$$

For derivations of eqns (6) and (7), see Simpson et al. (1996). If the Pr × EO interaction or EO main effect is present in a final model, then eqns (6) and (7) are applied separately for the first and second exposures. In calculating ED05 and ED50, q is prespecified as 0.05 and 0.50, respectively, in eqn (5). After plugging in MLEs from a final model, the threshold acoustic pressure x (*i.e.*, $p_{r(\text{in situ})}$) is either the unique solution to eqn (5) if Pr is the only significant effect in the final model, or a function

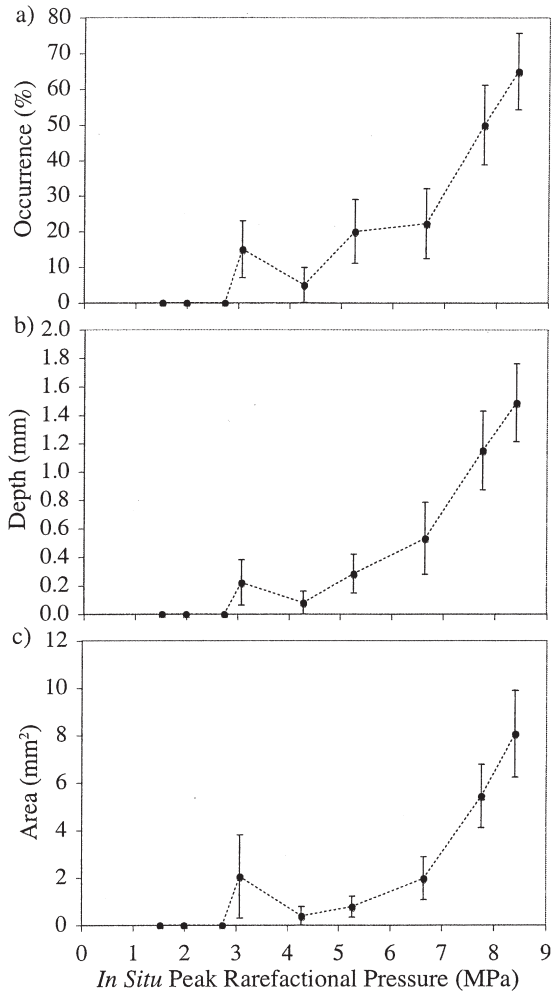

Fig. 2. (a) Lesion occurrence, (b) Lesion depth and (c) Lesion surface area as a function of the *in situ* peak rarefactional pressure. The dashed lines are straight lines connecting the mean values and are intended to provide graphical guidance. Error bars are the standard errors of the mean ($n = 20$ for each exposure condition except 6.65 MPa, for which $n = 18$).

of other significant effects otherwise. The standard errors for ED05 and ED50 are computed by first-order Taylor series approximations that are easily programmed in the R statistical language (Ihaka and Gentleman 1996).

RESULTS

Rabbit Threshold Estimation

In the US-induced lung hemorrhage study of rabbits (Fig. 2), the initial models (eqns (2) and (3)) for lesion occurrence and sizes each reduced to a simple final mixed model, where $p_{r(\text{in situ})}$ was the only significant effect (p-value < 0.0001) and the superthreshold slope estimate was positive: γ_1 for occurrence was estimated to be 0.39 with a standard error (SE) 0.09, β_1 for depth was 0.89 with a SE 0.16 and β_1 for root surface area was 1.29 with a SE 0.24. Neither probability of a lesion nor lesion size measurements in the rabbit study was found to be statistically dependent on the order of exposure after the effect of $p_{r(\text{in situ})}$ was considered. The mixed models did not detect a significant correlation between the two exposed lung sides on the same rabbit in either lesion occurrence (Est. a = 0.293, p-value = 0.545) or size measures (depth: Est. b = 0.255, p-value = 0.793; surface area: Est. b = 1.301, p-value = 0.911). This result agrees with the lack of within-animal correlation from the US-induced lung hemorrhage study in pigs that were also bilaterally exposed (O'Brien et al. 2003a).

The ED05 and ED50 thresholds from the binary lesion occurrence outcomes were estimated as described in the statistical methods section using eqns (5) and (6) because of the lack of significant interaction and order-of-exposure effects. Similarly, the ED05 and ED50 thresholds based on lesion size measures were estimated using eqns (5) and (7). Tables 2 and 3 report the ED05 and ED50 estimates with their standard errors based on the three final models for occurrence, depth and root surface area of lesions. The

Table 2. ED05 estimates (MPa) and SEs from lesion occurrence, depth and root surface area in rabbits, rats and mice.

Study	Occurrence	Depth	Root surface area
Rabbit threshold	3.43 (0.51)	3.37 (0.53)	3.18 (0.93)
Rat beamwidth*	3.4 (1.4)	2.4 (1.1)	3.9 (1.1)
Rat threshold†	2.80 (0.64)	2.63 (0.53)	2.95 (0.50)
Mouse threshold†	3.31 (0.61)	3.75 (0.46)	3.59 (0.45)

For the four studies under discussion, the center frequency was 5.6 MHz, beamwidth was 510 μm, exposure duration was 10 s, pulse repetition frequency was 1 kHz, and pulse duration was 1.1 μs for the rabbit threshold study and the rat beamwidth study and 1.2 μs for the rat and mouse threshold studies.

* From O'Brien et al. (2001b); † From Zachary et al. (2001a).

Table 3. ED50 estimates (MPa) and SEs for lesion occurrence, depth and root surface area in rabbits, rats and mice.

Study	Occurrence	Depth	Root surface area
Rabbit threshold	7.78 (0.45)	7.54 (0.41)	7.59 (0.44)
Rat beamwidth*	8.0 (1.4)	7.5 (1.2)	7.6 (1.2)
Rat threshold†	7.39 (0.37)	6.84 (0.33)	7.07 (0.31)
Mouse threshold†	7.89 (0.37)	7.96 (0.32)	7.71 (0.31)

For the four studies under discussion, the center frequency was 5.6 MHz, beamwidth was 510 μm, exposure duration was 10 s, pulse repetition frequency was 1 kHz and pulse duration was 1.1 μs for the rabbit threshold study and the rat beamwidth study and 1.2 μs for the rat and mouse threshold studies.

* From O'Brien et al. (2001b); † From Zachary et al. (2001a).

ED05 estimates in Table 2 for the rabbit threshold study were similar to each other across lesion occurrence (3.43 ± 0.51), depth (3.37 ± 0.53) and surface area (3.18 ± 0.93); so were the ED50 estimates in Table 3 for occurrence (7.78 ± 0.45), depth (7.54 ± 0.41) and surface area (7.59 ± 0.44). The consistency between the estimated thresholds from lesion occurrence, using eqn (6), and lesion sizes, using eqn (7), indicated the validity of the tobit regression model for lesion size for the purpose of estimating thresholds (O'Brien et al. 2003a).

Threshold Comparison in Rabbits, Rats and Mice

With threshold ultrasonic pressures now available for rabbits, it is interesting to compare them with the corresponding threshold estimates reported in the literature from similar US-induced lung hemorrhage studies in other small animals. In particular, Tables 2 and 3 summarize the estimated ED05s and ED50s, based on both occurrence and size of lesions, from four US-induced lung hemorrhage studies in three species by the same research group: these were the rabbit threshold study analyzed in this paper, the beamwidth study in rats (O'Brien et al. 2001b), the rat threshold study (Zachary et al. 2001a) and the mouse threshold study (Zachary et al. 2001a). Except for the rabbit threshold study, animals in the other three studies only had their left lung sides exposed. The rat beamwidth data were modeled by a logistic regression on lesion incidence and Gaussian tobit regressions on depth and root surface area (O'Brien et al. 2001b). The threshold estimates were extracted from Table 3 of O'Brien et al. (2001b) at beamwidth = 510 μm and center frequency = 5.6 MHz. In the rat threshold study and mouse threshold study, only the ED05s from the occurrence of lesions and the ED50s from the size measures were provided (Zachary et al. 2001a). For the purpose of comparison, these two datasets were reanalyzed by logistic regression models and tobit models and the corresponding ED05 and ED50 estimates can be found in Tables 2 and 3. As we are comparing threshold ultrasonic pressures across studies and species, it is important to note that the comparison is restricted to the ED05 or ED50 exposure levels at the same or similar exposure conditions: 5.6-MHz center frequency, 510-μm beamwidth, 10-s ED, 1-kHz PRF and 1.1-μs or 1.2-μs PD (1.1 μs for the rabbit threshold and rat beamwidth studies and 1.2 μs for the rat and mouse threshold studies).

Table 2 shows that the ED05 estimates are well contained in the ± (2 × SE) ranges (approximate 95% confidence intervals) of each other. The similarity of the ED05s within each row, that is, from the same study, was already verified by each separate study and it indicated the consistency of threshold estimation between a logistic regression and a tobit regression. The new finding here is that the thresholds in the same column for different species of animals are also within sampling error of each other. This pattern of consistency across species can be easily observed for lesion occurrence, depth and root surface area in Fig. 3, where, for each of the three outcome variables, the weighted average of the four estimated ED05s is marked by a vertical line and the 95% confidence interval for each estimate is represented by a solid horizontal line, with the estimate located at the center of the interval. All the horizontal lines are crossed with the associated vertical line, which shows that the 95% confidence intervals are overlapping and the threshold estimates are close to each other. It is interesting that the ED05s from the rabbit threshold study stay very close to the ED05s for rats and mice, even though the rabbits are much bigger than the rats and mice, as shown in Table 4. Table 4 also shows that the measured chest wall attenuation coefficient for rabbits is almost twice those for rats and mice.

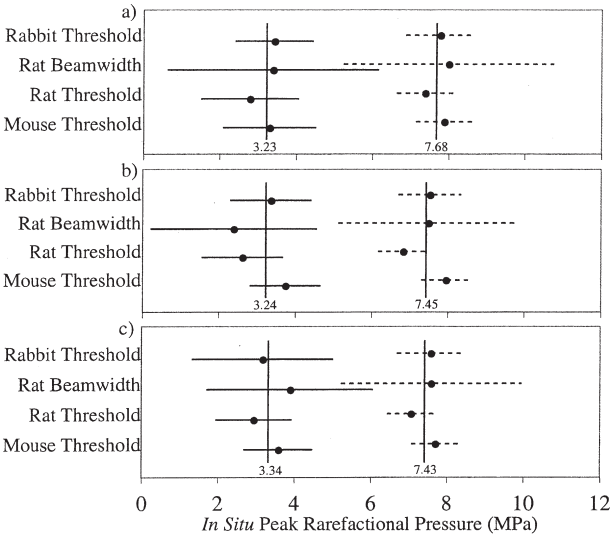

Fig. 3. Plots of 95% confidence intervals for the estimated ED05s (solid horizontal lines with the ED05 estimates located at the centers) and ED50s (dotted horizontal lines with the ED50 estimates located at the centers) based on (a) lesion occurrence, (b) lesion depth and (c) lesion area in rabbits, rats and mice. The x-axis indicates the *in situ* peak rarefactional pressure, and the y-axis displays the species and study name. The two vertical lines in each box represent the weighted averages of the ED05 and ED50 estimates, respectively, with the average values at the base of each vertical line. For each of the four studies, a common exposure regime was used: 5.6-MHz center frequency, 1-kHz PRF, 10-s ED and 510-μm beamwidth.

ED50 estimates can be found in Table 3 and similar results hold across different species as in the case of ED05s. Visual comparisons of the ED50s are given in Fig. 3, where dotted horizontal lines (side-by-side with

Table 4. Animal information for rabbits, rats and mice in the rabbit threshold study, rat beamwidth study, rat threshold study and mouse threshold study

Study	n	N	Age (d)	Weight (g)	Chest wall thickness (mm)	Chest wall attn. coef. (dB/mm)
Rabbit threshold	89	178	61∼88	1900∼2900	5.02∼6.78	1.02
Rat beamwidth*	144	144	72	220∼300	3.09∼4.32	0.59
Rat threshold†	160	160	72	190∼330	3.71∼5.96	0.59
Mouse threshold†	151	151	45	22∼32	1.94∼4.89	0.59

n denotes the number of animals in each study, and N gives the total number of observations. For the columns of age, weight and chest wall thickness, ranges of the variables are provided, as they are continuous.
* From O'Brien et al. (2001b); † From Zachary et al. (2001a).

the ED05s) depict the 95% confidence intervals. Note that, for lesion depth, the right end-point of the 95% confidence interval from the rat threshold study is 7.49 MPa, still greater than the weighted average of 7.45 MPa.

DISCUSSION

The objective of this study was to assess the threshold and superthreshold behavior of US-induced lung hemorrhage in adult rabbits, to gain greater understanding about species dependency. This is the first study that assessed lung hemorrhage thresholds in rabbits. Other species for which US-induced lung damage thresholds have been assessed include mouse (Child et al. 1990; Raeman et al. 1993, 1996; Frizzell et al. 1994; Dalecki et al. 1997b; Zachary et al. 2001a), rat (Holland et al. 1996; Zachary et al. 2001a; O'Brien et al. 2001b) and pig (Baggs et al. 1996; Dalecki et al. 1997a; O'Brien et al. 2003a).

Our experimental techniques and statistical approach (Simpson et al. 2004) for estimating US-induced lung damage thresholds have demonstrated great consistency across three species (*e.g.*, Fig. 3). Figure 4 shows all of our ED05 occurrence threshold findings across four species [mouse (Zachary et al. 2001a), rat (Zachary et al. 2001a; O'Brien et al. 2001b), rabbit (this study) and pig (O'Brien et al. 2003a)]. Pre-2000 occurrence threshold findings (Fig. 5) across three species [mouse (Child et al. 1990; Raeman et al. 1993; 1996; Frizzell et al. 1994; Dalecki et al. 1997b), rat (Holland et al. 1996) and pig (Baggs et al. 1996; Dalecki et al. 1997a)] have also been reported (AIUM 2000) for which experimental techniques and statistical approaches were different from ours. A principal difference between the two sets of studies lies in the exposure duration wherein our threshold findings used a 10-s ED (Fig. 4) to simulate incidental lung exposure, whereas the pre-2000 threshold findings (Fig. 5) used typically longer EDs. The 10-s ED studies yielded occurrence thresholds typically higher (median: 3.0 MPa; range: 1.2 to 5.8 MPa) than the pre-2000 thresholds (median: 1.0 MPa; range: 0.4 to 2.5 MPa).

Some general observations can be made from our occurrence ED05 findings (Fig. 4), because each of these studies was performed using the same experimental and analysis protocols and 10-s ED. The first group (151 adult ICR mice and 160 adult Sprague-Dawley rats) yielded no differences for either species or frequency. The second group (144 adult Sprague-Dawley rats) yielded no differences for either beamwidth or frequency. The third group (200 adult Sprague-Dawley rats) yielded a statistically significant trend for pulse duration. The fourth and fifth groups (323 cross-bred pigs divided into three age groups) found a significant age-dependent (although not monotonic) effect and further yielded a surprising finding that the more deflated lung was more sensitive to damage than was the more inflated lung. The sixth group (99 adult New Zealand White rabbits) yielded thresholds similar to those of mice and rats.

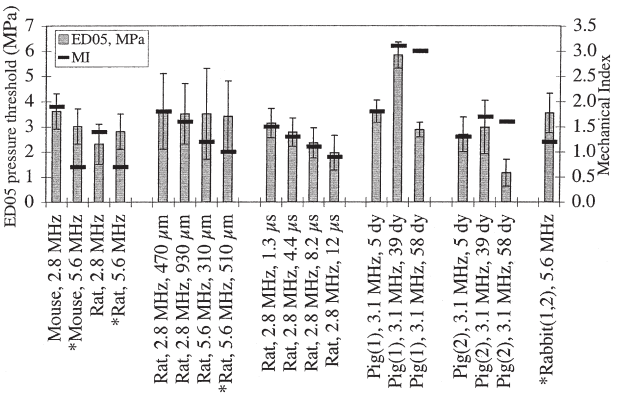

Fig. 4. Summary of ED05 occurrence thresholds in terms of $p_{r(in\ situ)}$ (MPa) (bars; left axis) and MI (lines, right axis). * denotes the studies that are evaluated in Tables 2, 3 and 4, and Fig. 3. Error bars are SEMs. These data, by groupings from left to right, are derived, respectively, from Zachary et al. (2001a), O'Brien et al. (2001b), O'Brien et al. (2003b), O'Brien et al. (2003a), O'Brien et al. (2003a), and this study.

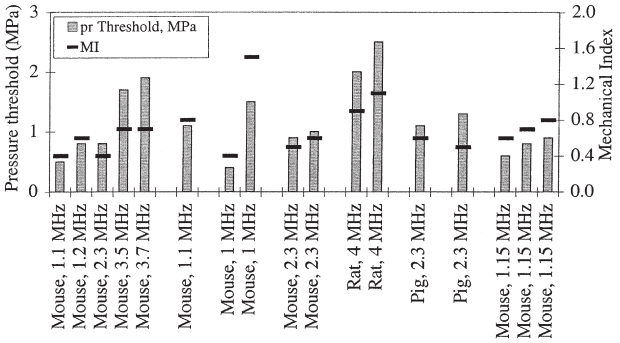

Fig. 5. Summary of occurrence thresholds in terms of $p_{r(in\ situ)}$ (MPa) (bars; left axis) and MI (lines, right axis) from studies not using our experimental techniques and statistical approach. These data, by groupings from left to right, are estimated, respectively, from Child et al. (1990), Raeman et al. (1993), Frizzell et al. (1994), Raeman et al. (1996), Holland et al. (1996), Baggs et al. (1996), Dalecki et al. (1997a) and Dalecki et al. (1997b).

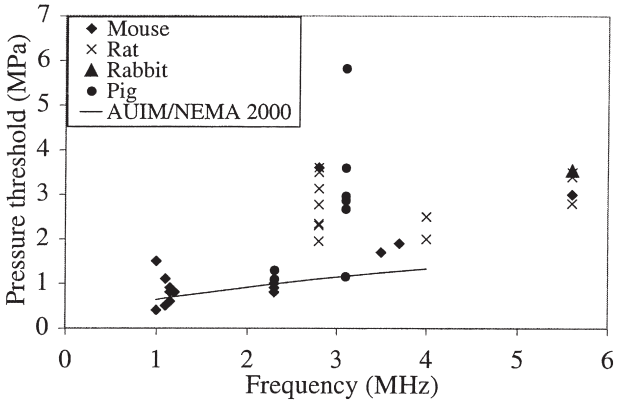

Fig. 6. Global summary of occurrence thresholds in terms of *in situ* peak rarefactional pressure as a function of frequency for four species (see Figs. 4 and 5) The solid line is the threshold equation derived from pre-2000 data (AIUM 2000).

In addition, other than two of the pig thresholds, all ED05s yielded MIs ≤1.9, the FDA (1997) regulatory limit, for all threshold studies except for the first-exposed pig lungs (fourth group). The explanation for the significant differences in the lesion thresholds for pigs might be the degree to which the lung is inflated at maximum expiration (O'Brien et al. 2002).

The MI was not a design variable in any of our studies; rather the *in situ* peak rarefactional pressure was the principal design variable and our analyses yielded the 5% threshold level based on the *in situ* peak rarefactional pressure. However, the MI must be reported and discussed for these findings because it is the quantity that is regulated by FDA (1997) and appears on the display of modern diagnostic US systems. Thus, our calibration procedures quantified the MI according to the specified measurement requirements (AIUM/NEMA 2004). The MI provides perspective to the clinical user about the levels used in our studies, that is, levels that are achievable by diagnostic US systems. Admittedly, the MI is a water-based quantity, not an *in vivo*-based quantity; the MI does not take into account the acoustic properties or the path length between the transducer and the tissue site of interest. Therefore, if a new regulatory peak value is to be developed, our findings also provide an experimental basis for why the MI may not be an appropriate regulatory quantity.

All of these occurrence threshold values (from Figs. 4 and 5) have been organized as a function of frequency (Fig. 6 relative to ultrasonic pressure and Fig. 7 relative to MI). Virtually every US-induced lung hemorrhage threshold is less than the FDA regulatory limit (MI <1.9, FDA 1997), that is, within the diagnostic US frequency range. These thresholds are over a wide range of animal weights [mouse: 22 to 32 g; rat: 190 to 330 g; rabbit: 1.9 to 2.9 kg; and pig: 1 to 25 kg] and chest wall thicknesses [mouse: 1.9 to 4.9 mm; rat: 4.1 to 6.0 mm; rabbit: 5.0 to 6.6 mm; and pig: 2 to 22 mm].

Also, the physiologic (Table 5) and morphologic (Table 6) properties of lung can be used to group or separate animal species. The critical structural features that can be used to separate species into distinct groups (Table 6) are pleural thickness (thin *vs.* thick), pleural blood supply (pulmonary artery *vs.* bronchial artery) and septal or interlobular connective tissue (scant *vs.* abundant). There are significant interspecies structural differences of the lungs, even when lungs and associated structures are evaluated at a subgross level (Plopper and Pinkerton 1992). Although all common mammalian species have parietal and visceral pleural surfaces, the thickness, vascularity and organization of the me-

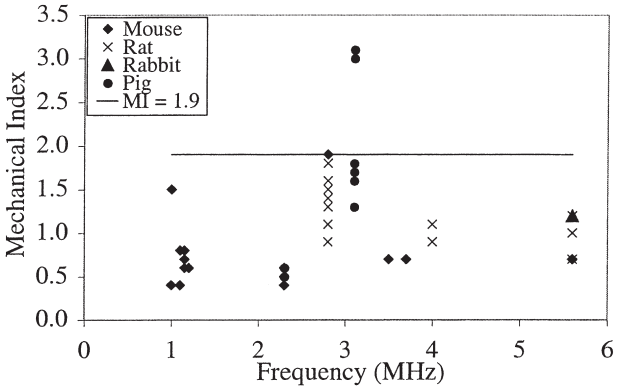

Fig. 7. Global summary of occurrence thresholds in terms of the MI as a function of frequency for four species (see Figs. 4 and 5). The solid line denotes an MI of 1.9, the FDA regulatory limit (FDA 1997).

Table 5. Lung properties for various adult mammalian species relative to the adult mouse (dash indicates that data could not be found)

Lung property	Adult mouse	Adult rat	Adult rabbit	Adult pig	Adult human
Total lung volume*,**,††	1	≈11	≈100	≈5000	≈6500
Alveolar surface area*,††	1	≈6	≈65	≈1500	≈1500
Mean alveoli diameter*,†,‡	1	≈1	≈2	≈2.3	≈5
Capillary surface area††	1	≈7.2	≈85	-	≈2300
Capillary volume††	1	≈6.6	≈95	-	≈2800
Lung compliance*,§,‖,#	1	≈11	≈175	≈750	≈4000

* Weibel (1971); † Tenney and Remmers (1963); ‡ Crosfill and Widdicombe (1961); § Hildebrandt and Young (1966); ‖ Ganong (1967); # Watson (1992); ** Sahebjami (1992); †† Pinkerton et al. (1992).

sothelium, submesothelial connective tissue and vascular system forming, in particular, the visceral pleura, vary between species, as do the extent and distribution of secondary septation with the lung and the distribution of connective tissue elements (Tyler and Julian 1992). In addition, the source of arterial blood to the visceral pleura varies between species (Table 6) and this distribution is linked to the "thinness" or "thickness" of the visceral pleura. On the basis of these comparisons, human beings can be clearly grouped closer to pigs (the "thick" group). When these same comparisons (Tables 5 and 6) are made between the "thick" group that contains human beings and pigs and with mice, rats and rabbits, it is clearly demonstrated that mice, rats and rabbits are in the "thin" group. Thus, there is a suggestion that these lung properties might weakly influence the US-induced lung hemorrhage, because the three thin group species (mice, rats and rabbits) have the same ED05s and ED50s (Figs. 3 and 4), whereas the ED05 of the thick group species (pig) tends to behave a bit differently (Fig. 4).

The results of our studies using mice, rats, rabbits and pigs have shown two important facts relative to the biologic mechanisms of damage: (1) there are no differences in biologic mechanism of injury induced by US based on species and age: therefore, structural differences among mammalian species studied are independent of the biologic mechanism that causes US-induced lung damage; and (2) US-induced lesions are similar in morphology in all species and age groups studied and the character of the lesions are independent of frequency, PRF and beamwidth, but not necessarily age. These findings suggest that the mechanism of injury is similar in all species and age groups. It is thus plausible to speculate that the same biologic mechanism causing US-induced lung hemorrhage in laboratory animals may be in play in human beings undergoing sonographic procedures with direct or incidental exposure of lung, especially patients with pulmonary disorders and "at risk" neonates. However, the extent of US-induced lung damage and the ability of the lung to heal (Zachary et al. 2001b) led to the conclusion that, although diagnostic US can produce lung damage at clinical levels, the degree of damage does not appear to be a significant medical problem.

Acknowledgements—This work was supported by NIH grant EB02641 (formerly HL58218) awarded to WDO and JFZ, and NSF grant DMS-0073044 awarded to DGS. We also thank P. Abrantes, T. Bigelow, J. Bredfeldt, Z. Hafez, M. Johnson, M. Oelze, R. Patel, P. Paul, M. Qayyum, S. Sakai, J. Schneider and B. Zierfuss for technical assistance.

Table 6. Comparative lung morphology (dash indicates that data could not be found)

Lung property	Mouse/rat/rabbit	Pig	Human
Pulmonary pleura size*	Thin	Thick	Thick
Pulmonary pleura blood supply*	Pulmonary artery	Bronchial artery	Bronchial artery
Interlobular and segmental connective tissue*	Little, if any	Extensive, interlobular surrounds many lobules completely	Extensive, interlobular partially surrounds many lobules
Pulmonary plural lymphatics*	Very few	Extensive	Extensive
Nonrespiratory bronchiole (nonalveolarized)*	Several generations	Several generations	Several generations
Respiratory bronchiole (alveolarized)*,†	Absent or single short generation	Absent or single short generation	Several generations
Terminal respiratory bronchiole*	Ends in alveolar ducts or very short respiratory bronchioles	Ends in alveolar ducts or very short respiratory bronchioles	Ends in respiratory bronchioles
Acinus transition zone*,†	Abrupt	—	Not abrupt

* Tyler and Julian (1992); † Pinkerton et al (1992).

REFERENCES

American Institute of Ultrasound in Medicine. Mechanical bioeffects from diagnostic ultrasound: AIUM consensus statements. J Ultrasound Med 2000;19:67–168.

American Institute of Ultrasound in Medicine and National Electrical Manufacturers Association. Acoustic output measurement standard for diagnostic ultrasound equipment. Laurel, MD and Rosslyn, VA, 1998.

American Institute of Ultrasound in Medicine and National Electrical Manufacturers Association. Standard for real-time display of thermal and mechanical acoustic output indices on diagnostic ultrasound equipment, Rev. 2. Laurel, MD and Rosslyn, VA, 2004.

Amemiya T. Tobit models: A survey. J Econometrics 1984;24:3–61.

Baggs R, Penney DP, Cox C, et al. Thresholds for ultrasonically induced lung hemorrhage in neonatal swine. Ultrasound Med Biol 1996;22:119–128.

Berk KN, Lachenbruch PA. Repeated measures with zeros. Stat Methods Med Res 2002;11:303–316.

Child SZ, Hartman CL, Schery LA, Carstensen EL. Lung damage from exposure to pulsed ultrasound. Ultrasound Med Biol 1990;16:817–825.

Crosfill ML, Widdicombe JG. Physical characteristics of the chest and lungs and the work of breathing in different mammalian species. J Physiol 1961;158:1–14.

Dalecki D, Child SZ, Raeman CH, Cox C, Carstensen EL. Ultrasonically induced lung hemorrhage in young swine. Ultrasound Med Biol 1997a;23:777–781.

Dalecki D, Child SZ, Raeman CH, et al. Age dependence of ultrasonically-induced lung hemorrhage in mice. Ultrasound Med Biol 1997b;23:767–776.

US Food and Drug Administration Use of mechanical index in place of spatial peak, pulse average intensity in determining substantial equivalence, Center for Devices and Radiological Health, FDA, Rockville, MD, April 14, 1994.

US Food and Drug Administration Information for Manufacturers Seeking Marketing Clearance of Diagnostic Ultrasound Systems and Transducers, Center for Devices and Radiological Health, FDA, Rockville, MD, September 30, 1997.

Frizzell LA, Chen E, Lee C. Effects of pulsed ultrasound on the mouse neonate: Hind limb paralysis and lung hemorrhage. Ultrasound Med Biol 1994;20:53–63.

Frizzell LA, O'Brien WD Jr., Zachary JF. Effect of pulse polarity and energy on ultrasound-induced lung hemorrhage in adult rats. J Acoust Soc Am 2003;113:2912–2926.

Ganong WF. Review of medical physiology. Los Altos, CA: Lange Medical Publications, 1967.

Harrison GH, Eddy HA, Wang JP, Liberman FZ. Microscopic lung alterations and reduction of respiration rate in insonated anesthetized swine. Ultrasound Med Biol 1995;21:981–983.

Hartman C, Child SZ, Mayer R, Schenk E, Carstensen EL. Lung damage from exposure to the fields of an electrohydraulic lithotripter. Ultrasound Med Biol 1990;16:675–683.

Hildebrandt J, Young AC. Anatomy and physics of respiration. In: Ruch TC, Patton HD (eds): Physiology and Biophysics. Philadelphia: W.B. Saunders, 1966:733–760

Holland CK, Deng CX, Apfel RE, Alderman JL, Fenandez LA, Taylor KJW. Direct evidence of cavitation in vivo from diagnostic ultrasound. Ultrasound Med Biol 1996;22:917–925.

Ihaka R, Gentleman R. A language for data analysis and graphics. J Computat Graphic Stat 1996;5:299–314.

Kramer JM, Waldrop TG, Frizzell LA, Zachary JF, O'Brien WD Jr Cardiopulmonary function in rats with lung hemorrhage induced by exposure to superthreshold pulsed ultrasound. J Ultrasound Med 2001;20:1197–1206.

Miller RJ, Frizzell LA, Zachary JF, O'Brien WD Jr Attenuation coefficient and propagation speed estimates of intercostal tissue as a function of pig age. IEEE Trans Ultrason Ferroelec Freq Contr 2002;49:1421–1429.

O'Brien WD Jr, Frizzell LA, Schaeffer DJ, Zachary JF. Superthreshold behavior of ultrasound induced lung hemorrhage in adult mice and rats: Role of pulse repetition frequency and pulse duration. Ultrasound Med Biol 2001a;27:267–277.

O'Brien WD Jr, Frizzell LA, Weigel RM, Zachary JF. Ultrasound-induced lung hemorrhage is not caused by inertial cavitation. J Acoust Soc Am 2000;108:1290–1297.

O'Brien WD Jr, Kramer JM, Waldrop TG, et al Ultrasound-induced lung hemorrhage: Role of acoustic boundary conditions at the pleural surface. J Acoust Soc Am 2002;111:1102–1109.

O'Brien WD Jr, Simpson DG, Frizzell LA, Zachary JF. Superthreshold behavior and threshold estimation of ultrasound-induced lung hemorrhage in adult rats: Role of beamwidth. IEEE Trans Ultrason Ferroelec Freq Contr 2001b;48:1695–1705.

O'Brien WD Jr, Simpson DG, Frizzell LA, Zachary JF. Threshold estimates and superthreshold behavior of ultrasound-induced lung hemorrhage in adult rats: Role of pulse duration. Ultrasound Med Biol 2003b;29:1625–1634.

O'Brien WD Jr, Simpson DG, Frizzell LA, Zachary JF. Superthreshold behavior of ultrasound-induced lung hemorrhage in adult rats: Role of pulse repetition frequency and pulse duration revisited. J Ultrasound Med 2005;24:339–348.

O'Brien WD Jr, Simpson DG, Ho M-H, Miller RJ, Frizzell LA, Zachary JF. Superthreshold behavior and threshold estimation of ultrasound-induced lung hemorrhage in pigs: Role of age dependency. IEEE Trans Ultrason Ferroelec Freq Contr 2003a;50:153–169.

O'Brien WD Jr, Zachary JF. Lung damage assessment from exposure to pulsed-wave ultrasound in the rabbit, mouse, and pig. IEEE Trans Ultrason Ferroelec Freq Contr 1997;44:473–485.

Penney DP, Schenk EA, Maltby K, Hartman-Raeman C, Child SZ, Carstensen EL. Morphologic effects of pulsed ultrasound in the lung. Ultrasound Med Biol 1993;19:127–135.

Pinheiro JC, Bates DM. Approximations to the log-likelihood function in nonlinear mixed effects models. J Computat Graphic Stat 1995; 4:12–35.

Pinkerton KE, Gehr P, Crapo JD. Architecture and cellular composition of the air-blood barrier. In: Parent RA (ed): Comparative Biology of the Normal Lung, vol 1. Boca Raton, FL: CRC Press, 1992:121–128.

Plopper CG, Pinkerton KE. Structural and cellular diversity of the mammalian respiratory system. In: Parent RA (ed): Comparative Biology of the Normal Lung, vol 1. Boca Raton, FL: CRC Press, 1992:1–5.

Raeman CH, Child SZ, Carstensen EL. Timing of exposures in ultrasonic hemorrhage of murine lung. Ultrasound Med Biol 1993;19: 507–512.

Raeman CH, Child SZ, Dalecki D, Cox C, Carstensen EL. Exposure-time dependence of the threshold for ultrasonically induced murine lung hemorrhage. Ultrasound Med Biol 1996;22:139–141.

Raum K, O'Brien WD Jr. Pulse-echo field distribution measurement technique of high-frequency ultrasound sources. IEEE Trans Ultrason Ferroelec Freq Contr 1997;44:810–815.

Sahebjhami H. Aging of the normal lung. In: Parent RA (ed): Comparative Biology of the Normal Lung, vol 1. Boca Raton, FL: CRC Press, 1992:351–366.

Sempsrott JM, O'Brien WD Jr. Experimental verification of acoustic saturation. Proceedings of the 1999 IEEE Ultrason Symp 1999: 1287–1290.

Simpson DG, Carroll RJ, Zhou H, Guth DL. Interval censoring and marginal analysis in ordinal regression. J Agricult Biol Environm Stat 1996;1:354–376.

Simpson DG, Ho M-H, Yang Y, Zhou J, Zachary JF, O'Brien WD Jr. Excess risk thresholds in ultrasound safety studies: Statistical methods for data on occurrence and size of lesions. Ultrasound Med Biol 2004;30:1289–1295.

Tarantal AF, Canfield DR. Ultrasound-induced lung hemorrhage in the monkey. Ultrasound Med Biol 1994;20:65–72.

Tenney SM, Remmers JE. Comparative quantitative morphology of the mammalian lung: Diffusing area. Nature 1963;197:54–56.

Teotico GA, Miller RJ, Frizzell LA, Zachary JF, O'Brien WD Jr. Attenuation coefficient estimates of mouse and rat chest wall. IEEE Trans Ultrason Ferroelec Freq Contr 2001;48:593–601.

Towa RT, Miller RJ, Frizzell LA, Zachary JF, O'Brien WD Jr Attenuation coefficient and propagation speed estimates of rat and pig intercostal tissue as a function of temperature. IEEE Trans Ultrason Ferroelec Freq Contr 2002;49:1411–1420.

Tyler WS, Julian MD. Gross and subgross anatomy of lungs, pleura, connective tissue septa, distal airways, and structural units. In: Parent RA (ed): Comparative Biology of the Normal Lung, vol 1. Boca Raton, FL: CRC Press, 1992:37–47.

Watson JW. Elastic, resistive, and inertial properties of the lung. In: Parent RA (ed): Comparative Biology of the Normal Lung, vol 1. Boca Raton, FL: CRC Press, 1992:175–216.

Weibel ER. Dimensions of the tracheobronchial tree and alveoli. In: Altman PL, Dittmer DS (eds): Biological Handbooks: Respiration and Circulation. Bethesda, MD: Federation of American Societies for Experimental Biology, 1971.

World Federation for Ultrasound in Medicine and Biology WFUMB symposium on safety of ultrasound in medicine: Issues and recommendations regarding non-thermal mechanisms for biological effects of ultrasound. J Ultrasound Med 1998;24:S1-S55:67–168.

Zachary JF, Frizzell LA, Norrell KS, Blue JP Jr, Miller RJ, O'Brien WD Jr. Temporal and spatial evaluation of lesion reparative responses following superthreshold exposure of rat lung to pulsed ultrasound. Ultrasound Med Biol 2001b;27:829–839.

Zachary JF, O'Brien WD Jr. Lung lesion induced by continuous- and pulsed-wave (diagnostic) ultrasound in mice, rabbits, and pigs. Vet Pathol 1995;32:43–45.

Zachary JF, Sempsrott JM, Frizzell LA, Simpson DG, O'Brien WD Jr Superthreshold behavior and threshold estimation of ultrasound-induced lung hemorrhage in adult mice and rats. IEEE Trans Ultrason Ferroelec Freq Contr 2001a;48:581–592.